Hybrid RANS/LES simulation of a supersonic coaxial He/Air jet experiment at various turbulent Lewis numbers

Lorris Charrier, Grégoire Pont, Simon Marié, Pierre Brenner, Francesco Grasso

Abstract In this article, the unstructured, high order finite-volume CFD solver FLUSEPA[1], developed by Airbus Safran Launchers, is used to simulate a supersonic coaxial Helium/Air mixing experiment. The aim is to assess the ability of the code to accurately represent mixing in compressible flows and to create a reference case in order to test a future hybrid RANS/LES (HRL) model with variable turbulent Prandtl and Schmidt numbers. Both RANS and HRL simulations are performed and the impact of Lewis number on the results is studied. Fine and coarse meshes are used to see the influence of spatial resolution on modeled and resolved scales. General good agreement is obtained for both RANS and HRL simulations. Predictably, the choice of Lewis numbers has almost no impact on the time-averaged fields of the fine HRL simulation. Its role is more significant on the coarse mesh and the steady RANS simulations.

1 Introduction

At high altitude, the large expansion of space launchers plumes can induce a massive flow separation in the boundary layer of the fuselage. The resulting recirculation bubble can mix and react with the supersonic hot plume, containing unburnt

Lorris Charrier, Simon Marié, Francesco Grasso
ENSAM DynFluid, 151 Boulevard de l'Hopital 75013 Paris, France,
e-mail: lorris.charrier@ensam.eu,
e-mail: simon.marie@cnam.fr,
e-mail: francesco.grasso@cnam.eu

Lorris Charrier, Grégoire Pont, Pierre Brenner
Airbus Safran Launchers, 66 route de Verneuil 78130 Les Mureaux, France,
e-mail: lorris.charrier@airbusafran-launchers.com,
e-mail: gregoire.pont@airbusafran-launchers.com,
e-mail: pierre.brenner@airbusafran-launchers.com

[1] Registered trademark in France with number 134009261

fuel, and bring very hot gas upwind of the base. During the development of a new launcher, the prediction of the behavior of this kind of flow is primordial. Moreover, its highly unsteady character cannot be predicted correctly by RANS simulations. As a result the use of LES or HRL models is necessary and the effects of unresolved scales on resolved ones need to be modeled.

In most cases this is done thanks to an additional turbulent contribution in the diffusive term of conservation equations. Turbulent diffusion coefficients for energy and species mass fraction are often linked to turbulent momentum diffusion coefficient (turbulent eddy viscosity) by constant non-dimensional ratios (turbulent Prandtl and Schmidt numbers). Numerous RANS simulations demonstrated that turbulent Prandtl and Schmidt numbers are in fact non-constant and have a strong impact on the results [1]. Some improved models have been developed to address this issue and show promising results [14, 7]. With an approach very similar to $k-\varepsilon$ turbulence model, additional transport equations for unresolved enthalpy (or energy) variance and sum of species mass fraction variance are introduced to compute turbulent thermal diffusivity and turbulent mass diffusion coefficient.

In non-reacting LES, constant turbulent Prandtl and Schmidt number hypothesis is generally sufficient for most of the transport is carried by large-scale structures. In the case of reactive LES, turbulence at the smallest scales play a key role in the reaction. An extension of the variable Prandtl/Schmidt number model to HRL may contribute to gain additional information about sub-filter energy and mass fraction variance in LES-resolved zones and could be exploited for modeling turbulence/chemistry interactions.

In the present paper, we focus on a case that will be used to evaluate the performance of the future variable hybrid Prandtl/Schmidt model. As a first step we carried out unsteady simulations of supersonic coaxial Helium/air jet mixing based on Cutler *et al.* experiment [10] by using the unstructured, high order finite-volume CFD solver FLUSEPA, developed by Airbus Safran Launchers. A recently implemented DDES $k-\varepsilon$ turbulence model is used. The influence of constant turbulent Lewis number hypothesis, defined as the ratio between turbulent Schmidt and Prandtl numbers, analyzed and the results are compared with the data. Two meshes are used to study the impact of spatial resolution. Results are fair to good, depending on the mesh and turbulent Lewis numbers chosen.

2 FLUSEPA SOLVER

FLUSEPA is a high order unstructured finite volume CFD code for the modeling of highly compressible, turbulent, viscous and reactive flows with particles over complex geometries in relative motion. One of the main features of FLUSEPA is its CHIMERA-like conservative method that avoid interpolation at grids intersection thus maintaining the same order [11, 4, 5, 6]. The code allows different parts of the geometry to be meshed independently and then to assemble them in a single composite grid by merging the resulting meshes of geometric intersection[2].

2.1 Turbulence modeling

The Reynolds stress tensor is modeled with a Boussinesq eddy viscosity assumption [3]. In the present simulation we have used a high Reynolds $k-\varepsilon$ RANS model [8] and a high Reynolds $k-\varepsilon$ Delayed Detached Eddy Simulation (DDES) HRL model [13]. In this case, the turbulent viscosity μ_t is decreased by making the dissipation term of the turbulent kinetic energy d_k sensitive to grid in vortex-dominated regions and out of the boundary layer. The model takes the maximum between the RANS classical dissipation term $\rho\varepsilon$ and a LES term calculated with a local characteristic length scale Δ

$$d_k = \rho \max\left(\varepsilon; \frac{k^{3/2}}{C_{DES}\Delta}\right) \tag{1}$$

The turbulent heat flux is modeled through a Fourier-like approximation with a turbulent thermal conductivity (λ_t). The species turbulent diffusive flux tensor uses a Fickian-like model introducing a turbulent diffusion coefficient (D_t). Both are calculated from constant turbulent eddy viscosity and constant Prandtl/Lewis number hypothesis.

$$\lambda_t = \frac{C_p \mu_t}{Pr_t} \tag{2}$$

$$D_t = \frac{\lambda_t}{\rho C_p Le_t} \tag{3}$$

2.2 Numerical scheme

Convective fluxes are calculated by using the Godunov algorithm that gives the exact solution to Riemann problems. A high-order k-exact MUSCL[3] approach is used for reconstruction of variables into cells. In the following simulations a 3rd order spatial upwind scheme, with local 4th order accurate non-dissipative recentering method is used. The blending function between upwind and centered scheme is based on an analytic criterion that ensures stability [12]. Explicit temporal integration is done with a 2nd order Heun scheme along with a local adaptive time stepping algorithm. This method regroups cells into different temporal levels, each one having its own timestep, to minimize the CPU consumption[4]. An advanced 1st order accurate Euler scheme is used for implicit temporal integration in RANS simulations.

[2] Higher priority level meshes overlapping those of lower priority

[3] Monotonic Upstream-Centered Scheme for Conservation Laws

[4] It involves several iteration for small cells and few for big ones

3 Description of the test case

The experiment selected is the one by Cutler *et al.* at NASA Langley research center, specifically designed for CFD code validation. It features Schlieren visualization, Pitot pressure, total temperature, gas composition surveys along with a precise instantaneous non-intrusive RELIEF velocimetry at various locations [10].

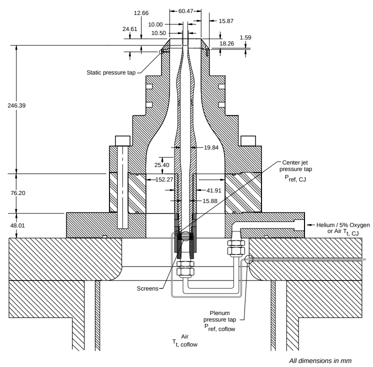

Fig. 1: Experimental setup schematic [10]

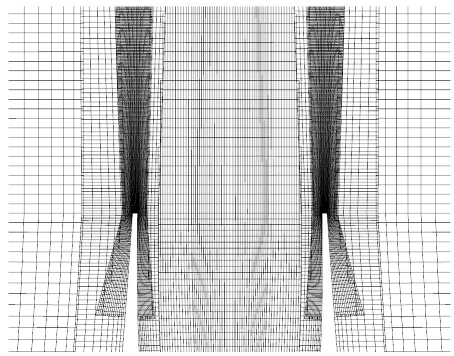

Fig. 2: Overlapping meshes example. The fine LES-optimized mesh overlaps the background RANS-optimized mesh with a "buffer" mesh layer to reduce the jump in cell size at the intersection

The experimental facility, illustrated in Fig. 1, consists of two coaxial axisymmetric bodies. The inner and outer body diameters are 10 and 60.47 mm, respectively. The inner jet is composed of 95% He and 5% O_2 (necessary for RELIEF velocimetry); outer jet is made of air. Both jets discharge in quiet atmosphere. Central and coaxial Mach number are identical and equal to 1.8. Because of the high sound speed of Helium, the center jet is more than twice as fast as the air jet. The convective Mach number is 0.7.

In our simulations, all meshes take advantage of the conservative intersection strategy. A coarse RANS-optimized mesh is used for steady simulations that features a large part of the internal geometry of nozzles to ensure a proper development of the boundary layers. The domain extends up to 250 (inner) jet diameters downstream and 140 jet diameters radially. y^+ are comprised between 30 and 300 and standard wall function are used. The azimuthal resolution of the far field is 120 cells. The total number of cells of the RANS-optimized mesh is near 3 million.

For HRL simulations, the same mesh is used as a "background" and several different overlapping meshes can be added to increase spatial resolution specifically in zones dominated by turbulence. This allows to drastically reduce the number of cells compared with classical HRL meshes. In our simulations, we used LES-optimized meshes in the primary mixing region ()between central and outer jet) and in the secondary mixing region ()between outer jet and quiet atmosphere). The LES-optimized meshes have been chosen to include all the mixing region delimited by boundaries of 1% and 99% center jet molar fraction described in the experiment. An example of overlapping meshes on primary mixing region can be seen on Fig. 2. Two different sets of overlapping meshes are tested. The "fine" one features a radial resolution of 40 cells and a maximum azimuthal resolution of 240 cells in both mixing regions. In the axial directions, overlapping meshes are chosen to ensure quasi-isotropy of cell sizes and extends up to 25 jet diameters. The total number of cells is approximately 14 million. The "coarse" overlapping meshes set is the same as the "fine" one with a resolution divided by two in all directions. It contains 5 million cells. As a result, the impact of sub-filter scale modeling on resolved flow is expected to be more visible.

4 Simulation results

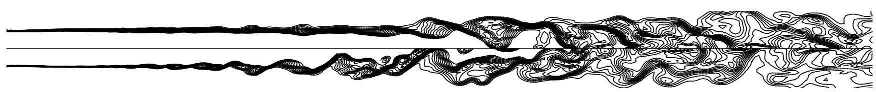

Fig. 3: Isocontour of Helium mass fraction showing differences of mixing layer development between $Le_t = 1$ (up) and $Le_t = 1.5$ (down) coarse HRL cases.

Fig. 4: Isocontour of Helium mass fraction showing differences of structures resolution between fine (up) and coarse (down) $Le_t = 1.5$ HRL cases.

The radial distribution of time-averaged axial velocity plots at numerous axial position and turbulent Lewis number is shown is Fig. 5. The results are in general good agreement with experiment. At intermediate axial locations, fine HRL cases give better results than RANS and coarse HRL. However, at large distances from nozzle exit simulations consistently underestimate the axial velocity. An opposite tendency is observed in RANS simulations. As expected, the influence of turbulent Lewis number on time-averaged velocity is almost nonexistent for the fine-grid HRL case and rather small for RANS case. Coarse HRL results are more counter-intuitive. $Le_t = 0.5$ and $Le_t = 1.5$ cases give similar outcomes that are comprised between RANS and fine HRL results but $Le_t = 1$ simulation presents a significantly larger time-averaged axial velocity in the jet core. Observation of temporal evolution of the velocity at various locations over the sampling period does not show any transient behavior.

Time-averaged root-mean-square (RMS) fluctuations of axial velocity at the same locations are reported in Fig. 5. It has been calculated taking into account unresolved contributions estimated from the modeled turbulent kinetic energy on the assumption of quasi-isotropic turbulence at sub-filter scale levels

$$\langle U_{rms} \rangle \approx \sqrt{\langle \tilde{U}'^2 + \frac{2}{3}\tilde{k} \rangle}. \tag{4}$$

where $\langle \cdot \rangle$ denotes time-averaging operator, $\tilde{\cdot}$ represents the Favre filtering and $\tilde{U}' = \tilde{U} - \langle \tilde{U} \rangle$. For RANS simulations, only the contribution of $\tilde{k}$ remains. We can observe that the order of magnitude of fluctuations is well predicted. Estimation of RANS time-averaged U_{rms} gives good results far from the nozzles where the turbulent structures are more isotropic. This assumption is not realistic near the splitter tip, which could explain the under-prediction of RMS fluctuations at the first survey positions. At intermediate distances, the mixing layer width seems to be underestimated. This is coherent with the over-estimation of center-jet velocity. RANS RMS velocity fluctuation estimations do not show a great sensitivity to turbulent Lewis number. Once again we observe that the coarse HRL simulations are more sensitive, and particularly the $Le_t = 1$ case. We can observe that the mixing layer development of this case is delayed compared to the others. Comparison of instantaneous fields shows that in the first part of the flow, the cells count in the mixing layer is near the limit of resolution of turbulent structures allowed by our numerical scheme[5]. The slight difference caused by value of Lewis number seems to be enough to yield a noticeable influence on the position of resolution of first vortices, impacting the whole mixing layer development, as seen in Fig. 3. The fine HRL results are generally in good agreement with experiment. An over-prediction of peak amplitude at intermediate positions is observed, however, the mixing layer growth is better predicted than in RANS and coarse HRL cases. The influence of turbulent Lewis number is barely noticeable for this mesh. The present results do not show the dip which is visible in the experiment at $x = 82$ mm[6]. This is likely to be ascribed to reflection/refraction of shocks/expansion waves in the mixing layer that locally affects turbulence and this issue was also found in previous RANS, LES, and HRL simulations of this case [10, 2, 9].

In the Fig. 6 we report the comparison of the radial distribution of the time-averaged He-O_2 mixture molar fraction (95 % He + 5 % O_2) at various axial positions. For the RANS simulations, we can observe that $Le_t = 1$ gives the closest results from experiment. This is consistent with previous computations of this flow. For both HRL, spreading of He-O_2 mixture seems underestimated, however fine HRL case performs better than coarse HRL at jet outer limits. The influence of turbulent Lewis number on unsteady cases is less critical than for time-averaged axial velocity and RMS fluctuations.

In the Fig. 6 we also report the comparison of the radial distribution of the time-averaged pitot pressure, normalized by coflow pressure, with experiment. We have

[5] Thanks to the 4th order local recentering method FLUSEPA can resolve vortices with 6 cells in diameter

[6] Similar drops in experimental RMS fluctuations are also visible at $x = 62$ and $x = 102$ mm, not printed on this paper.

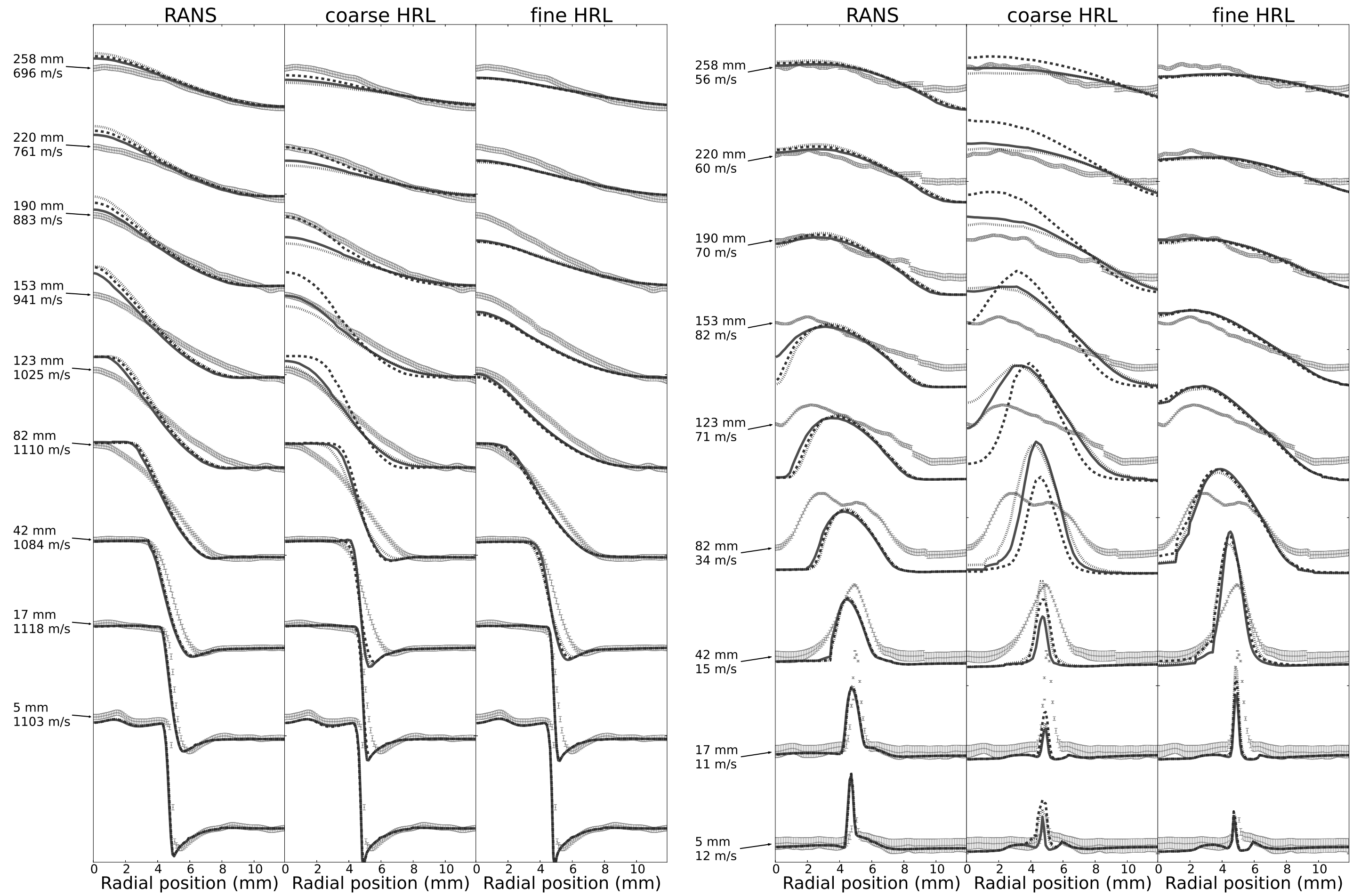

Fig. 5: Comparison between experimental and computed time-averaged axial velocity (left) and RMS fluctuations (right) for the three cases. Circles with errorbars : experiment, solid line : $Le_t = 0.5$ simulation, dash : $Le_t = 1$ simulation, dots : $Le_t = 1.5$ simulation. Each curve is shifted from the precedent position. Position of survey and centerline value indicated on left.

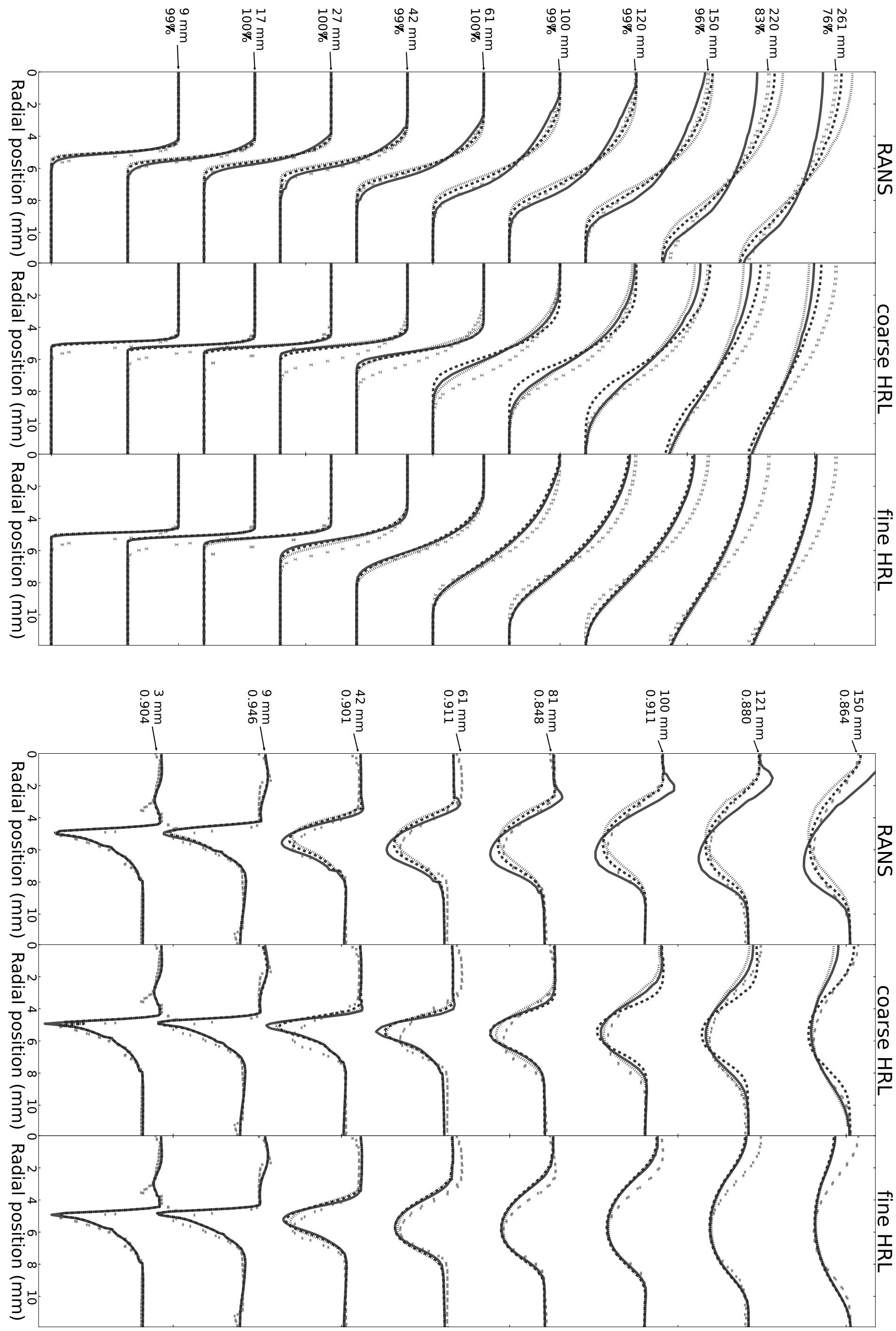

Fig. 6: Comparison between experimental and computed time-averaged center jet initial molar fraction (left) and normalized pitot pressure (right) for the three cases. Circles with errorbars : experiment, solid line : $Le_t = 0.5$ simulation, dash : $Le_t = 1$ simulation, dots : $Le_t = 1.5$ simulation. Each curve is shifted from the precedent position. Position of survey and centerline value indicated on left.

general good agreement with Cutler survey, especially in the first half of the probed zone. Fine HRL case results are particularly close from experiment excepted for the underestimated centerline pitot pressure at the last survey axial positions. Additional experimental error could result from the intrusive character of pitot probes.

5 Conclusion

FLUSEPA CFD code has been used to simulate a compressible coaxial mixing jet experiment [10]. The influence of mesh resolution and turbulent Lewis number on steady RANS and Hybrid RANS/LES simulations was studied. Results for RANS and fine mesh HRL computations are satisfying. RANS results for He-O_2 field are good when a correct turbulent Lewis number is selected. According to [10], differences between experiment and simulation for axial velocity and its RMS fluctuation could be reduced by increasing the radial diffusion of turbulent kinetic energy. These two observations make the RANS simulations dependent on model constants. HRL computations on the fine mesh do not present sensitivity to turbulent Lewis number and give better results for RMS fluctuations of axial velocity. By resolving a large part of the turbulence, it becomes less dependent of the sub-filter modeling in the mixing region. Results for the coarse HRL cases are mitigated. Mesh resolution is barely sufficient to resolve largest vortices in the mixing layer. As a consequence, the position of the firsts Kelvin-Helmholtz structures may be very sensitive to small variations of flow characteristics. This could explain why the mixing layer development is delayed in the $Le_t = 1$ case. The coarse set of simulations shows that HRL computations may be dependent on model constants and give worst results than RANS for time-averaged variables when mesh is not suitable. In the future, these results will be used as comparison for the validation of a HRL version of a variable turbulent Prandtl/Schmidt number model. The additional variables, describing sub-filter sum of mass fraction variance and sub-filter energy variance in LES-resolved zones, will be used to model turbulent/chemistry interactions at unresolved scales.

References

1. R. A. Baurle. Modeling of high-speed reacting flows : established practices and future challenges. *AIAA*, 267, 2004.
2. R.A. Baurle and J.R. Edwards. Hybrid reynolds-averaged/large eddy simulations of a coaxial supersonic freejet experiment. *AIAA journal*, 48:(551–571), 2010.
3. J.V Boussinesq. Essai sur la théorie des eaux courantes. *Mémoire des savants étrangers, Académie des sciences de Paris*, 1877.
4. Pierre Brenner. Three dimensional aerodynamics with moving bodies applied to solid propellant. *27th Joint Propulsion Conference, Sacramento, USA*, 1991.
5. Pierre Brenner. Simulation du mouvement relatif de corps soumis a un écoulement instationnaire par une méthode de chavauchement de maillage. In *AGARD conference proceedings 578 : Progress and challenges in CFD methods and Algotithms, Seville, Spain*, 1995.
6. Pierre Brenner. A conservative overlapover grid method to simulate tocket stage separation. In *3rd symposium on overset composite grid and solution technology, Los Alamos*, 1996.
7. K.W. Brinckman, W.H. Calhoon Jr, and S.M. Dash. Scalar fluctuation modeling for high-speed aeropropulsive flows. *AIAA journal*, 45:(1036–1046), 2007.
8. S. Catris and B. Aupoix. Density corrections for turbulence models. *Aerospace Science Technologies*, 4:1–11, 2000.
9. Peter Cocks. *Large eddy simulation of supersonic combustion with application to scramjet engines*. PhD thesis, University of Cambridge, 2011.
10. A.D. Cutler, G.S. Diskin, J.P. Drummond, and J.A. White. Supersonic coaxial jet experiment for computational fluid dynamics code validation. *AIAA journal*, 44:(585–592), 2006.
11. G. Monge. *Géométrie Descriptive*. PARIS, BAUDOUIN, Imprimeur du Corps lgislatif et de linstitut national, AN VII (1799)., 1799.
12. Grégoire Pont. *Self adaptive turbulence models for unsteady compressible flows*. PhD thesis, Arts et Méters ParisTech, Airbus Defense & Space, 2015.
13. M Strelets. Detached eddy simulation of massively separated flows. In *AIAA, Aerospace Sciences Meeting and Exhibit, 39 th, Reno, NV*, 2001.
14. X. Xiao, H.A. Hassan, and R.A. Baurle. Modeling scramjet flows with variable turbulent prandtl and schmidt numbers. *AIAA journal*, 45:(1415–1423), 2007.